PRACTICES, PITFALLS AND GUIDELINES IN VISUALISING LAGRANGIAN OCEAN ANALYSES

C. Kehl [a,b]*, R.P.B. Fischer [a], E. van Sebille [a]

[a] Utrecht University, Institute for Marine and Atmospheric Research, Princetonplein 5, NL-3584 CC Utrecht
{c.kehl; r.p.b.fischer; e.vansebille}@uu.nl
[b] Utrecht University, Department for Information and Computing Sciences, , Princetonplein 5, NL-3584 CC Utrecht

Commission IV, WG IV/9

KEY WORDS: Visualisation design, Visual guidelines, Lagrangian analysis, Oceanography, IPCC visual style guide

ABSTRACT:

The Lagrangian analysis of particulate matter, biota and drifters, which are dispersed by turbulent fluid currents, is a cornerstone of oceanographic studies, covering diverse study objectives. The results of Lagrangian simulations and observations is predominantly visualised by means of easy-access plotting interfaces and simple presentation techniques. We analysed over 50 publications from the years 2010-2020 with respect to their visual design to deduce common visualisation practices in the domain. Individual figures are analysed towards adherence to visualisation best-practices, algebraic visualisation guidelines and the IPCC visual style guide. In this article, we present the resulting best-practices and common pitfalls in the design of Lagrangian ocean visualisations. Based on this visual study, we highlight that raising awareness of established visual guidelines may have a higher impact on improving the visual quality of publications in oceanography than the vigorous development of more general-purpose visualisation tools.

1. INTRODUCTION

The dispersal and transport of objects by ocean currents, as well as their physical, biological and chemical response to changing environmental conditions, is studied via Lagrangian analysis- and simulation approaches. Such analysis improves the understanding of phenomena such as fish migration (Schilling et al., 2020), plankton sedimentation (Dämmer et al., 2020, Nooteboom et al., 2020), nutrient transport (Cetina-Heredia et al., 2018), the transport of plastics and other micro-particulates as well as the source-to-sink interaction between rivers and beaches (Kaandorp et al., 2020), shallow waters, the deep sea and the ocean floor (Nooteboom et al., 2019). This study approach is different to Eulerian approaches, which are mainly used to study global interactions between the oceans, the atmosphere and the climate, in that its major focus is on the transport patterns of individual floating- or submerged groups of objects (e.g. tracers) within the fluid-flow domain.

The outcomes of Lagrangian ocean simulations are important for stakeholders, decision-makers, non-governmental agencies (NGOs), inter-governmental panels (e.g the Inter-governmental Panel on Climate Change (IPCC)) and governmental institutions to plan and enact policies for environmental protection, fishing, as well as climate change mitigation strategies. As such, the simulation results need to be visually communicated to the (potentially) non-expert audience via plots and graphics. Statistical infographics are commonplace and often well-understood due to the semi-standardized structure by the audience. In contrast, the visualisation of the results in their geospatial context quickly become complex and require a good structure as well as an optimal utilisation of visualisation tools and concepts to convey the intended message of the study.

In our work, we observe a large discrepancy between the available plotting interfaces (Hunter, 2007) and dedicated visualisation tools (Ahrens et al., 2005, Schroeder et al., 2004), the comprised perceptual knowledge on (geo-)visualisation, for example (Brewer et al., 2003, MacEachren and Taylor, 2013), and the actually applied practices for visualising Lagrangian studies in the literature. This paper intends to close the gap between the available knowledge, the technical possibilities and their still-limited application in oceanic studies. In this respect, we (a) analyse and structure the (oceanographic) literature record in a taxonomy of study objectives and intents, visual techniques and visual elements, then (b) discuss common practices and combinations within the taxonomy to highlight advantageous and disadvantageous visualisation approaches, from which *best-practice* guidelines and *visual pitfalls* emerge. Furthermore, we discuss (c) the methods of algebraic visualisation (Kindlmann and Scheidegger, 2014) and the IPCC visual style guide (Gomis et al., 2018) as self-evaluation guidelines for researchers for authoring visual material in Lagrangian ocean analysis. Lastly, we demonstrate on one examples the impact and change of applying those guidelines for the improvement of visualisations in this domain. The focus of this analysis is specifically on the perceptual aspects of the visualisation that apply to almost all Lagrangian ocean visualisations in recent literature, neglecting aspects and limitations already imposed on prior stages of those studies, e.g. the simulation. As such, available data and computational feasibility already impose limits on scale, maximum fidelity and specifications of the ocean general circulation model (OGCM) on the simulation. Naturally, those aspects carry over to the visualisation, while in fact being design choices of prior modelling stages. Additionally, visualisation aspects such as projection and transformation, sample resolution, as well as data smoothing, filtering and rendering interpolation impact the visualisation result. Those aspects are of technical rather than perceptual nature, and hence also not specifically discussed in this paper.

* Corresponding author

2. STUDY OBJECTIVES IN LAGRANGIAN OCEAN ANALYSIS

Lagrangian simulations and analyses are applied to a diversity of study areas and issues in oceanography. Traditionally, physical oceanography studies the behaviour and responses of oceanic fluids on *velocities* (Abernathey et al., 2016) and its derivative properties, such as *vorticity* (de Marez et al., 2020, Zhang et al., 2020), *eddy formation* (Abernathey et al., 2010, Nooteboom et al., 2020), *turbulence* (Zhang et al., 2020), *divergence*, finite-time Lyapunov exponent (FTLE) and finite-size Lyapunov exponent (FSLE) (Falk et al., 2014). We comprise in our study the velocity-related aspects under the *velocity model*, examples of which are numerous in literature (see overview in (van Sebille et al., 2018)).

As a result of the different velocity- and flow regimes, oceanographers can detect *coherent structures*, i.e. large fluid bodies with homogeneous flow properties. Examples of those are, on a small scale, Lagrangian coherent structures (LCSs) (Haller, 2015, Wichmann et al., 2021), and oceanic basins on a larger scale (Wichmann et al., 2019a, Wichmann et al., 2020). The gain of a Lagrangian approach is the quantification of the connectivity between the basins, hence extracting trends between flow origins- and destinations.

Lagrangian (oceanic) flow simulation thus model the transport of objects in fluids, hence extracting *trajectories* of the objects moved by the fluid (e.g. (van Sebille et al., 2019). Those objects can represent biota (e.g. fish (Schilling et al., 2020) or plankton (Dämmer et al., 2020, Nooteboom et al., 2020)), plastics (Duncan et al., 2018, Onink et al., 2019, van Sebille et al., 2020) or real-world analogue *drifters* (Wichmann et al., 2020). Some of those quantities can be of microscopic scale, referred to as *particulate*, whereas all those transported objects are digitally simulated as *particles* in a particles system. Henceforth, *particles* refer to the digital object model whereas *particulates* refer to the physical, microscopic objects. An overview of what Lagrangian ocean particles can represent is given in (van Sebille et al., 2018).

Objects and particulates in the ocean are subject to a source-to-sink behaviour (Kaandorp et al., 2020), where objects emerge from the source (e.g. rivers, antropogenic ejection), move within the oceans, and then settle (temporarily- or permanently) in a sink (e.g. ocean floor, beaches). The source-to-sink cycle, on the example of plastic litter, is explained in (van Sebille et al., 2020). Modelling the source-to-sink behaviour is captured in Lagrangian simulations by what we will refer to as the *lifetime model*, which encompasses effects such as origin, capture, beaching and sediment deposition (Nooteboom et al., 2019).

The modelled Lagrangian particles are more than just motion objects, which is why visualising Lagrangian simulations also goes beyond traditional fluid-flow visualisation, as in (Post and Van Walsum, 1993, Van Wijk, 2002). The particles are commonly used as *tracers* to quantify the *density* of a fluid property, such as litter density (van Sebille et al., 2018), or the concentration of a physical-, biological- or chemical property, such as nutrients (Cetina-Heredia et al., 2018) and algae (Lobelle et al., 2021) via the *particle density*, in which case the particle density is used as precursor for the actual trajectories. Additionally, tracing the property change along a particle's modelled lifetime gives insight into the evolution of the property over time. The property's evolution over a particle's trajectory further grants insight into the connectivity of different particles types, which can represent different biota species (Busch et al., 2020).

Lagrangian models require Eulerian flow fields as input for particle advection in the fluid. In oceanography, those Eulerian models refer to OGCMs, which are published at discrete scales (e.g. NEMO (Madec et al., 2017)). Quantifying the effect of this modelling detail on particle dispersion is a further study focus in Lagrangian ocean analysis (Nooteboom et al., 2020). A related physical aspect of increasing importance is *particulate matter dispersion* and *diffusive*- and *stochastic* modelling to capture motion uncertainty that takes effect below the discretely modelled scale of an OGCM (Berloff and McWilliams, 2002, Shah et al., 2011).

All the outlined study objectives require appropriate visualisation to communicate the modelled effects, results and insights to the audience, where the communication goal is either *information*, the demand for *action* or the inclusion of the new knowledge into policies & procedures. The visualisations need to adhere to common perceptual guidelines (as provided by the visualisation literature body (Tufte, 2001, Brewer et al., 2003, Munzner, 2014)), though they are often neglected in current publication practice. An important aspect in every geo-visualisation is the provision of the spatial context, which relates to the representation of adjacent topography or the underlying bathymetry in the plots.

3. TAXONOMY FOR LAGRANGIAN OCEAN VISUALISATION

In this paper, we propose a visual taxonomy to provide guidelines specific to the diverse study objectives explained in section 2. From the literature outline follows a taxonomy for the individual study objectives and their communication intents, presented in fig. 1. Here, LCSs and basin analysis is grouped in one, as the goal is communicating clustered structures within the ocean. Secondly, visualising uncertainty within the simulation results is a distinct topic in literature. Uncertainty in Lagrangian simulations emerges from various sources, of which scale artifacts, particle diffusion, fluid mixing and error margin assessments are representative examples. The composition of the lifetime model and the velocity model is discussed above (section 2), as is the the use of tracers. While the presentation of particle densities is often intended to quantify a tracer concentration, e.g. (Schilling et al., 2020) displaying larvae-particle density, it can also be visualised as trajectory precursor, as in (Van Sebille et al., 2012). In other words, instead of plotting whole particle trajectories and showing the advection process, particle densities simply show the state of a particle set P at any time t_x, where the trajectory is the integration of all time state $\int_{t=0}^{T} p\epsilon P$ of one particle instance. Representative examples for particle-particle connectivity, source-to-sink connections and inter-structure connectivity are rare in literature.

3.1 Categorisation of visual tools & techniques

On the overview of the techniques (fig. 1), we first highlight the difference between *plotting* and actual *image composition* and appreciate that some elaborate visualisation techniques go beyond what simple plotting interfaces (e.g. gnuplot, matplotlib, and their many derivatives) can offer. This difference leads to the split between common practices by domain experts and the available toolset: domain experts frequently maximise the visual output quality of plotting interfaces due to the interfaces'

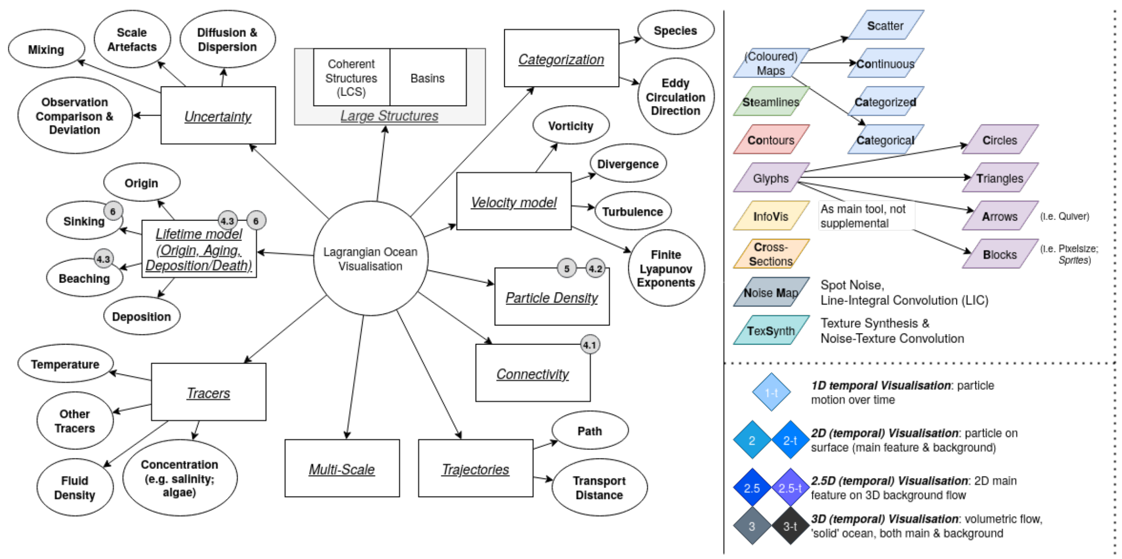

Figure 1. Taxonomy for Lagrangian ocean analysis study objectives (left), visualisation techniques (mid-top), graphical dimensions (mid bottom) and visual channels (right). Info-bubbles attached to individual study objective boxes indicate the sections in this article in which those subjects are discussed by example.

easy access, whereas actual image composition and associated techniques is required compound plots and renderings of complex data relationships, as well as the representation of multivariate data. Open-access course notes on *visualisation* as base-articles as (Post and Van Walsum, 1993, Schroeder et al., 2004) provide further details.

The elements in this overview are well-known and long-time demonstrated in fluid-flow visualisation (Post and Van Walsum, 1993). Colour maps are adapted for semantic and thematic representations, and oceanography-specific, perceptually-guided colour maps have been proposed in literature (Thyng et al., 2016). Glyph-based visualisation (Borgo et al., 2013) is increasingly common for Lagrangian ocean visualisation, be it in form of arrows (i.e. *hedgehog-* or *quiver* plot), (transparent) circles or pixel blocks (i.e. *sprites*) for pointsize-adapted particle positions. Cross-section plots are still prevalent in Lagrangian oceanography literature, due to the absence of applying image composition and 3D rendering. Novel techniques such as *texture synthesis* (Khlebnikov et al., 2012) have been proposed for (Eulerian) ocean visualisation in the visualisation community, extending traditional proposals of line-integral convolution (LIC)- or spot *noise maps* (Van Wijk, 2002), though they are underutilized in the oceanography community.

3.2 Categorisation of graphical dimensions, visual variables & visual channels

The above-listed techniques are the tools to maps the digital data to a given layout. The visualisation literature highlights that creating a data visualisation via selecting channels and variables is more appropriate then a straight technique application without prior visual design (Munzner, 2014). Hence, the overview of visual channels (fig. 1) follows established literature (Tufte, 2001, Brewer et al., 2003, Munzner, 2014). Regarding the graphical dimensions (fig. 1), we highlight the abundance of temporal-1D (1D-t) plots (e.g. depth-trajectory cross-sections), 2D plots and temporal 2D (2D-t) plots (as multifigure image panels) in the oceanography literature. Notable exceptions from the norm are found temporal 2.5D Paraview plots[1] and custom oceanographic 3D renderings (e.g. (Raith et al., 2017)).

[1] Uriel Zajaczkovski's scientific youtube channel - `https://www.youtube.com/user/urielzaja/videos`

4. VISUALISATION PRACTICES FROM THE LITERATURE

Using the above-outlined taxonomy, we compare figures from the available literature on selected case studies that display common intents to show different approaches for visual communication. Thus, the common intend of the studies is the selecting criterion of the displayed examples.

To visualise all Lagrangian data in the spatial context, the particle trajectories can be shown in their entirety as line plots. Because this large amount of dense information leads to clutter and occlusion, the main message can often be captured better with a compressed, alternative design.

4.1 Connectivity

A first study intent and visual output is to show the basin connectivity by connecting the initial and final particle positions over the simulation's timespan. Based on a particle's lifetime, this shows the basin connectivity and the integrated, dispersive characteristics of specific regions in the study area. The examples of (Wichmann et al., 2020) (fig. 2(a)) and (Wichmann et al., 2019b) (fig. 2(b)) illustrate these connections via sprite- or circular glyphs representing the particle locations, coloured by categorical hues to identify the movement between coherent regions.

The use of circular glyphs reduces the clutter in contrast to streamline trajectories. Instead, common plotting tools lack support for customising glyphs of individual particles, resulting in glyph occlusion that obscures detailed information. The glyph size and transparency can be adapted among the visual channels to overcome occlusion. Reducing the glyph size allows for a fine-grained plot, at the risk for individual particles to drop below the printed resolution (i.e. dots per inch (dpi)). This effect can be seen in figure 2(b), hence limiting the practicality of glyph size modulation. Introducing transparent glyphs is hence more promising to represent overlapping data. The

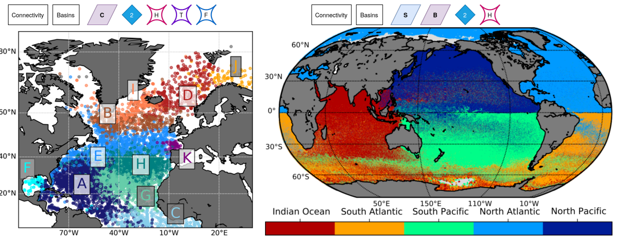

(a) (b)

Figure 2. Basin connectivity - mapping initial to final locations. a) (Wichmann et al., 2020), fig. 6 (adapted), transparent glyphs. b) (Wichmann et al., 2019b), fig. 3c (adapted), dense scatter plot

transparent glyphs in figure 2(a) allow overlapping glyphs to be recognised as more opaque regions. The solid edge of the glyphs reduce the amount of visible overlap.

For the geospatial context, the landmasses are shown together with the marine data. Both studies colour the landmass in neutral grey that differs in saturation from the data and in brightness from the oceanic background i.e. no data). Both figures include black contours for the coastline, which could have been omitted since it can distract from the displayed main-feature information.

In addition to common caveats of alpha composition (discussion in sec. 5), the hue composition may lead to issues in fig. 2. The coherent regions are distinguished by categorical hues in both figures. Although hue is a strong visual cue, the number of categories in both figures, seven and eleven respectively, are the limit of reasonably distinguishable hues per image (Bianco et al., 2015). To improve the differentiation of the hues, the adjacent colours should be *complementary colours*. In figure 2(b), the hues are well distributed to provide contrast, though orange and yellow sources are hard to distinguish, as are North Pacific particles entering the Atlantic through the Suez canal. In figure 2(a), the blue tones in the south are very similar, and the browns and reds are hard to distinguish in the north. The reason of the colour distribution is the cluster separation: similarly coloured clusters are more closely related in the network. The major cluster split is between the Subtropical Gyre (blue tones) and the Subpolar Gyre (red tones). Here, perhaps the message of the figure is not to show the integrated movement, but highlighting the dissimilarity between individual clusters.

4.2 Particle density

A second commonly mapped particulate quantity of global ocean studies is particle density, demonstrating their accumulation in specific regions. These plots can be interpreted as 2D histograms, mapping the particle set size to colours.

Figures 3(a) and 3(b) both employ coloured bins to map the amount of particles on the global surface ocean. The employed colour maps differ: Figure 3(a) uses monochromatic saturation whereas figure 3(b) uses both hue and brightness. Since the spectral sequence of hues does not inherently encode quantitative values, using only hues prevents the reader from interpreting the data intuitively. The use of saturation or brightness can encode quantities more naturally. The high red-hue saturation in figure 3(a) can easily be connected to the density of particles. Similarly, the yellow-hue brightness in figure 3(b) can be associated with a high intensity, leading to high *visual-data correspondence*.

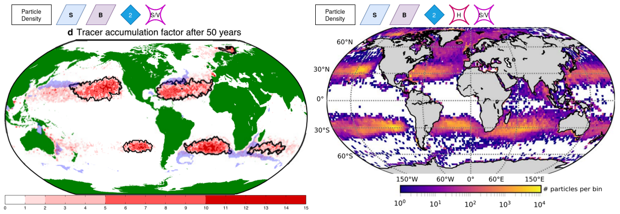

(a) (b)

Figure 3. Particle densities. a) (Van Sebille et al., 2012), fig. 1 (adapted), monochromatic saturation and significant-value dark contour highlight. b) (Wichmann et al., 2019a), fig. 1 (adapted), hues and brightness.

We can take the argument one step further by looking at the representation of *no-data*-values. In both figures this is represented by the white background colour. To follow the logic in the data, the *no-data*-value value corresponds here to the zero-value, which should coincide with the colour mapping. In figure 3(a) this is well done as the lower quantities are desaturated to match the white background.

4.3 Lifetime model - coastal origin and beaching

As humans occupy the continents, oceanographic processes that most immediately impact the public take place at the coast. The waste products that end up in the ocean come from the rivers and people in general are most bothered by pollution if it ends up on beaches. Where other oceanographic data require a 2D cartographic visualisation, coastal particle data is currently 1D.

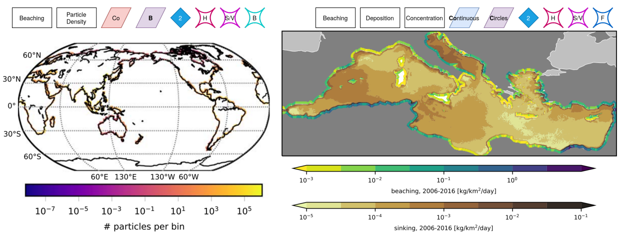

(a) (b)

Figure 4. Coastline data. a) (Wichmann et al., 2019a), fig. 7, Initial particle positions. b) (Kaandorp et al., 2020), fig. 4, Particles ending their trajectory on the coast.

Figures 4(a) and 4(b) show origin- and beached deposition particle counts at the coast. Both figures use colour maps that cycle sequentially through both hue and brightness. The main difference is the visualisation of the actual coastline and the neighbouring domains. In figure 4(a), the coastline itself is depicted with a black contours without further graphical difference between the oceans and land. In figure 4(b), the coastline is not depicted, as it is already clear from the beaching data where it is located. Co-plotting a secondary dataset (here: amount of sinking debris per day) in the oceans domain provides sufficient yet subtle visual contrast to separates the ocean and land domains.

5. COMMON VISUAL PITFALLS

Adherence to perceptual principles of visualisation design is important in order to preserve interpretation coherence between the author and the readership. Non-adherence to the perceptual principles leads to visualisation pitfalls that, in the end, limit the interpretability of the visualisation by the reader or contrasts the scientific statements given in-text. Thus, visualisation pitfalls are an avoidable source of interpretation disagreement between the author and the readership. In this section, we focus on the prevalent aspects in visualisations of Lagrangian oceanographic literature. By analysing 52 oceanographic publications (2010-2020), certain common pitfalls emerge aside the illustrated examples above.

Continuous and categorised coloured maps, together with sprite scatter plots, form the basis of most visualisations. Whereas early publications excessively employ *jet-map* colour scales, we observe a change toward the *viridis*- and *plasma* colour scales in recent articles[2]. Still, employing single-hue colour scales and thus leaving the *hue* channel for supplementary data is often neglected. Generally, *hue* is over-employed as visual channel, straining the viewers attention while limiting the potential for co-plotting context information.

A specific pitfall of sprite-based scatter plots is the mismatch between the basemap's background colour and the zero-information point of the employed colour map. This fails, according to algebraic visualisation (Kindlmann and Scheidegger, 2014), *visual-data correspondence*, which literature states as one of the most common colour mapping errors.

As shown in fig. 2(a) and 2(b), plotting particle locations via *solid or semi-transparent glyphs* is increasingly utilised for Lagrangian ocean visualisations. Their increased application is not only due to technical improvements of common plotting software, but also because the glyphs are scale-adapted on print-outs. Glyph size modulation can reduce occlusion and clutter in cases where transparency modulation is not possible for technical reasons. Glyph scatterplots support, in contrast to gridded- or meshed base maps, space-adaptive plotting that is decoupled from a predefined resolution. That said, a common pitfall in visualisations that use adaptive transparency is the *failure to the invariance principle*, saying that the visual depiction needs to be invariant to the underlying data organisation. Failures to the principle are commonly back-tracked to an ordering-problem (fig. 5): plotting a list of N particles as semi-transparent circle-glyph will result in different plots for (a) a sequential traversal order, (b) a random traversal order, or (c) a longitude-latitude traversal order. The glyph is combined with another attribute (e.g the basin indicator in fig. 2(a)), and hence the plot needs to be ordered towards this primary glyph attribute to achieve *plot invariance*. Additionally, authors should be aware of the interplay between opacity, saturation, brightness and background. A high opacity fully saturates an image pixel with few overlapping particles . A low opacity makes sparsely-distributed glyphs hardly visible, especially on a bright background. Better visibility of transparent glyphs on dark background is due to the high contrast perception of the human-visual spectrum (Tufte, 2001). Moreover, modulating transparency and brightness results in the same tone mapping and thus should be mutually-exclusive.

On the subject of trajectory plots, also often referred to as *spaghetti plots*, they contribute particularly to Lagrangian simulations when co-plotting the lifetime- and the velocity model of the analysis. The major drawback is the rapidly-occurring visual clutter with an increased number and length of trajectories. It gives a good impression of the overall chaotic nature of the fluid transport, but due to the visual clutter it prevents

[2] Named colourmaps illustrated in *matplotlib* - `https://matplotlib.org/stable/tutorials/colors/colormaps.html`

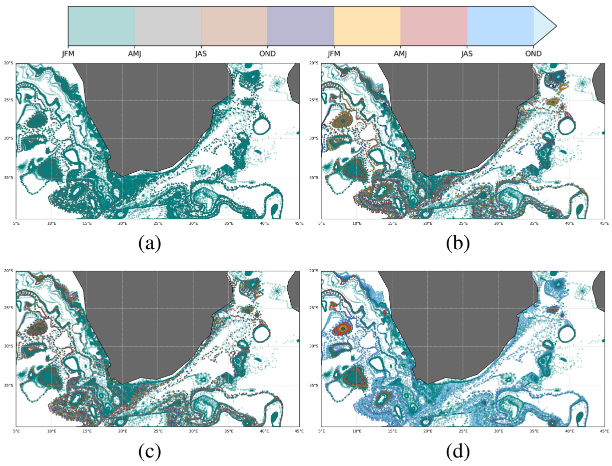

Figure 5. Illustration of the alpha-ordering problem: the plot shows particle densities similar to fig. 2(a), the individual particles are stored in random order. Plotting the data sequentially (as stored) can yield a highly-ordered (a) or arbitrary (b) alpha composition that occludes data points. Random permutation of the plotting order (c) only partially alleviates the issue. Ordering the data (d) according to the main feature (here: start observation season) yields replicable, reliable plots with minimal alpha-occlusion of the main feature.

any quantitative or qualitative assessment of the figure. Trivial solutions are to plot just a constrained subset of trajectories or a selected timescale, though then shifting the responsibility to trajectory selection, which is not possible to perform *á priori*. A better insight into trajectory structure would be gained by bundling spatially-adjacent trajectories (see (Lhuillier et al., 2017) for technical details) in a preprocessing step. Alternatively, the use of animation (snapshots) of particle traces (see (Post and Van Walsum, 1993) will gain more prominence in the community. Furthermore, animations are a simple way to prevent a common failure to the correspondence principle (Kindlmann and Scheidegger, 2014) for trajectories: they are often plotted without start-/end indicator, thus plotting the trajectory front-to-back leads to the same figure as plotting back-to-front.

We illustrate the design process of improving Lagrangian ocean visualisations on a recent collaboration with D.M.A. Lobelle, who plots in her article (Lobelle et al., 2021) the sinking timescale of biofouled plastic depending on the particulate size. The starting plot (fig. 6) shows the timescales on a value-decreasing colour map, whereas the plotted timescale actually increases. This contradiction complicates the figure interpretation. Furthermore, due to the decaying colour value and contrast, variations in the last third of the colour scale hard to distinguish.

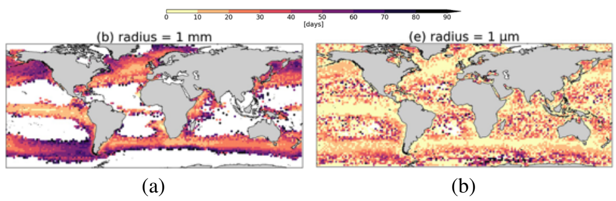

Figure 6. Initial scatter-plot depiction for sinking timescales of biofouled plastics by D.M.A. Lobelle.

We collectively improved the colourmap. First, to increase the distinctiveness and visibly of higher values (i.e. long sinking timescales), the colourmap is inverted. This allows a more fine-grained distinction of high values (see fig. 7(b), southern Antarctic region) while preserving sufficient contrast for small sinking timescales (see fig. 7(a), mid-Atlantic area). The resulting dark base-tone was counter-acted by compressing the lower end of the colour scale (see fig. 8(a)) or by switching to a gridded glyph-plot (fig. 8(b)).

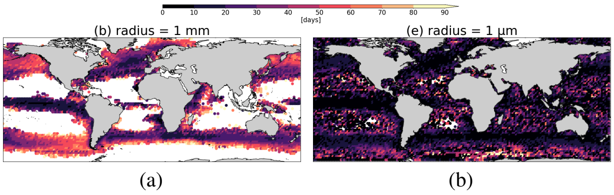

Figure 7. Inverting the colour map gives more prominence to peak-values in the plot, compared to fig. 6

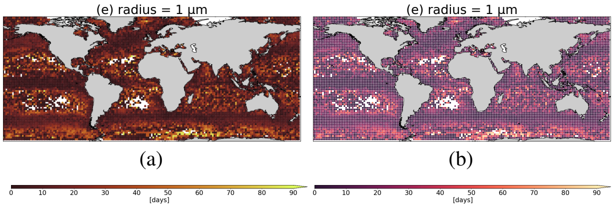

Figure 8. Counter-acting the dark base-tone of the plot for overall short sinking timescales by (a) shrinking the lower-end scale of the colour map or (b) plotting a gridded scatterplot with circular glyphs.

The result gridded, circular-glyph scatterplot iteration conversely decreases the figure contrast again that was attempted to be gained. Hence, the compressed colour map can be inverted to counter-act the contrast loss. This then leads to the above-described issue of *invariance principle failure*: the background colour (white) is colour-wise closest to lower-end colour map values (i.e. small timescales), hinting that all none-plotted areas have sinking timescales too small to depict. This contradicts simulation results, as none-plotted areas have sinking timescales far exceeding the simulated timespan. The solution of the design was to (a) using the original colourmap while shortening the colour span of the last-third, resulting in higher distinctiveness of long timescales, and (b) choosing a dark (black) basemap background to correctly express the semantics of *no-date areas*. The resulting figures in the article correctly depict the data while avoiding visibility-, contrast- and visual interpretation issues (see fig. 9).

6. VISUALISATION GUIDELINES FOR LAGRANGIAN OCEAN ANALYSIS

A guideline for the visual authorship of Lagrangian ocean analysis results can be used in multiple stages of the process, for example as sanity checklist before article submission, as reference for structuring the visual storyline during the writing process, or even as visual design guide earlier during the analysis phases.

A first stage of guideline is checking that the common pitfalls outlined in section 5 are avoided. Using the proposed taxonomy above helps organising (a) what study objective is being covered

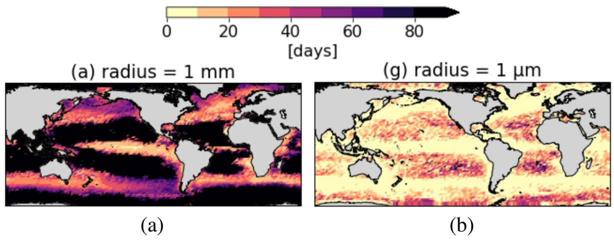

Figure 9. Final iteration of the visualisation with (i) shortened last-third of the colour scale and (ii) dark base tone to adhere to the invariance principle, reprint from (Lobelle et al., 2021), fig. 1 © The sinking timescale Copyright 2020, D.M.A. Lobelle

and (b) what channels are used to represent which data attribute. Those attributes can also be implicit, e.g. the trajectory is an accumulation of particles locations over time, though time may not be explicitly stored. Those defined visual parameters help reviewing the figure in order to minimise amount of visual channels and to use subtle visual cues while avoiding the listed pitfalls.

Our main approach is the use of algebraic visualisation as guideline. Algebraic visualisation (Kindlmann and Scheidegger, 2014) not only describes design principles in mathematical, reproducible language, it also describes common problems of element ordering, colour map choices, glyphs design, and their common resolution. The mathematical structure as well as discussed examples (e.g. hedgehog plots, scatter plots, continuous maps) make the approach well applicable to studies in physical oceanography.

Thematically, a further applicable guideline is the IPCC visual style guide (Gomis et al., 2018). The style guide already comprises the knowledge from milestone visualisation literature, such as (Tufte, 2001), (Brewer et al., 2003), (Munzner, 2014) and (Kindlmann and Scheidegger, 2014), into a comprehensible guideline for geo-visual authorship of environmental research. If further represents the guidelines by which the IPCC selects and re-authors (if so required) images and articles when including them in the stakeholder- and committee reports. It therefore shows the practical implications of adhering or opposing the accepted visual practices. The style guide itself includes a clear binary-tree questionnaire guidelines, which is intended as a reference for authors when preparing their publishing material.

7. CONCLUSION

This article discussed common practices in the visualisation of Lagrangian ocean analysis, structured around taxonomy of *study intents*, *visual techniques* and visual *dimensions, variables and channels*. Using this taxonomy and available guidelines for algebraic visualisation, visual design fundamentals and the IPCC visual style guide, best practices and common pitfalls were analysed on specific examples from the literature.

The article demonstrates the variety of visual designs in the target domain. We see from the examples and the analysis that simple permutations and modifications in the visual channels and variables can yield an improved understanding of the figure - notably within the already existing software framework of plotting interfaces (e.g. matplotlib). That said, visualising certain *compound objectives*, such as the velocity model together with concentrations or particle densities, can quickly reach the limit of simple plotting interfaces. In those instances, more accessible software that allows custom *(layered) image composition* or *custom rendering* is required to create clean, unambiguous visualisations. Prototype examples of such techniques are listed in the literature overview, though currently remain hard to access for the oceanographic community.

Conversely, reviewing the available practices, it may not be the development of novel software and tools that significantly improve Lagrangian ocean visualisations, but rather the raising of awareness of existing visual design principles and guidelines within the community, which will boost the clarity of published visualisations among domains experts as well as its comprehension by the target audience outside the physics- and oceanographic domain.

ACKNOWLEDGEMENTS

The two head authors created the taxonomy and its application in tandem, with continuous iterative feedback of E. van Sebille. All authors thank the OceanParcels group of Utrecht University's IMAU and its close, related partners for their graphics contribution. The research is supported by the "Tracking Of Plastic In Our Seas" (TOPIOS) project (grant agreement no. 715386) and partly by the IMMERSE project (grant agreement no. 821926), both funded by ERC's Horizon 2020 Research and Innovation program. A majority of the outlined studies were performed in the Parcels framework (Delandmeter and van Sebille, 2019).

REFERENCES

Abernathey, R., Marshall, J., Mazloff, M., Shuckburgh, E., 2010. Enhancement of Mesoscale Eddy Stirring at Steering Levels in the Southern Ocean. *Journal of Physical Oceanography*, 40(1), 170 - 184.

Abernathey, R. P., Cerovecki, I., Holland, P. R., Newsom, E., Mazloff, M., Talley, L. D., 2016. Water-mass transformation by sea ice in the upper branch of the Southern Ocean overturning. *Nature Geoscience*, 9(8), 596–601.

Ahrens, J., Geveci, B., Law, C., 2005. Paraview: An end-user tool for large data visualization. *The visualization handbook*, 717(8).

Berloff, P. S., McWilliams, J. C., 2002. Material transport in oceanic gyres. Part II: Hierarchy of stochastic models. *Journal of Physical Oceanography*, 32(3), 797–830.

Bianco, S., Gasparini, F., Schettini, R., 2015. Color coding for data visualization. *Encyclopedia of Information Science and Technology, Third Edition*, IGI Global, 1682–1691.

Borgo, R., Kehrer, J., Chung, D. H., Maguire, E., Laramee, R. S., Hauser, H., Ward, M., Chen, M., 2013. Glyph-based visualization: Foundations, design guidelines, techniques and applications. *Eurographics (STARs)*, 39–63.

Brewer, C. A., Hatchard, G. W., Harrower, M. A., 2003. ColorBrewer in print: a catalog of color schemes for maps. *Cartography and geographic information science*, 30(1), 5–32.

Busch, K., Taboada, S., Riesgo, A., Koutsouveli, V., Ros, P., Cristobo, J., Franke, A., Getzlaff, K., Schmidt, C., Biastoch, A., Hentschel, U., 2020. Population connectivity of fan-shaped sponge holobionts in the deep Cantabrian Sea. *Deep Sea Research Part I: Oceanographic Research Papers*, 103427.

Cetina-Heredia, P., van Sebille, E., Matear, R. J., Roughan, M., 2018. Nitrate Sources, Supply, and Phytoplankton Growth in the Great Australian Bight: An Eulerian-Lagrangian Modeling Approach. *Journal of Geophysical Research: Oceans*, 123(2), 759-772.

Dämmer, L. K., de Nooijer, L., van Sebille, E., Haak, J. G., Reichart, G.-J., 2020. Evaluation of oxygen isotopes and trace elements in planktonic foraminifera from the Mediterranean Sea as recorders of seawater oxygen isotopes and salinity. *Climate of the Past*, 16(6), 2401–2414.

de Marez, C., Carton, X., Corrard, S., L'Hgaret, P., Morvan, M., 2020. Observations of a Deep Submesoscale Cyclonic Vortex intheArabian Sea. *Geophysical Research Letters*, 47(13), e2020GL087881. e2020GL087881 10.1029/2020GL087881.

Delandmeter, P., van Sebille, E., 2019. The Parcels v2.0 Lagrangian framework: new field interpolation schemes. *Geoscientific Model Development*, 12(8), 3571–3584.

Duncan, E. M., Arrowsmith, J., Bain, C., Broderick, A. C., Lee, J., Metcalfe, K., Pikesley, S. K., Snape, R. T., van Sebille, E., Godley, B. J., 2018. The true depth of the Mediterranean plastic problem: Extreme microplastic pollution on marine turtle nesting beaches in Cyprus. *Marine Pollution Bulletin*, 136, 334 - 340.

Falk, M., Seizinger, A., Sadlo, F., Üffinger, M., Weiskopf, D., 2014. Trajectory-augmented visualization of lagrangian coherent structures in unsteady flow. *International Symposium on Flow Visualization (ISFV14), Daegu, Korea*.

Gomis, M. I., Pidcock, R. et al., 2018. Ipcc visual style guide for authors. techreport, IPCC WGI Technical Support Unit.

Haller, G., 2015. Lagrangian coherent structures. *Annual Review of Fluid Mechanics*, 47, 137–162.

Hunter, J. D., 2007. Matplotlib: A 2D graphics environment. *IEEE Annals of the History of Computing*, 9(03), 90–95.

Kaandorp, M. L. A., Dijkstra, H. A., van Sebille, E., 2020. Closing the Mediterranean Marine Floating Plastic Mass Budget: Inverse Modeling of Sources and Sinks. *Environmental Science & Technology*, 54(19), 11980-11989. PMID: 32852202.

Khlebnikov, R., Kainz, B., Steinberger, M., Streit, M., Schmalstieg, D., 2012. Procedural Texture Synthesis for Zoom-Independent Visualization of Multivariate Data. *Computer Graphics Forum*, 31(3pt4), 1355-1364.

Kindlmann, G., Scheidegger, C., 2014. An Algebraic Process for Visualization Design. *IEEE Transactions on Visualization and Computer Graphics*, 20(12), 2181-2190.

Lhuillier, A., Hurter, C., Telea, A., 2017. State of the Art in Edge and Trail Bundling Techniques. *Computer Graphics Forum*, 36(3), 619-645.

Lobelle, D., Kooi, M., Koelmans, A. A., Laufkötter, C., Jongedijk, C. E., Kehl, C., van Sebille, E., 2021. Global modeled sinking characteristics of biofouled microplastic. *Journal of Geophysical Research: Oceans*, 126, e2020JC017098.

MacEachren, A., Taylor, D., 2013. *Visualization in Modern Cartography*. ISSN, Elsevier Science.

Madec, G., Bourdallé-Badie, R., Bouttier, P.-A., Bricaud, C., Bruciaferri, D., Calvert, D., Chanut, J., Clementi, E., Coward, A., Delrosso, D. et al., 2017. NEMO ocean engine.

Munzner, T., 2014. *Visualization analysis and design*. CRC press.

Nooteboom, P. D., Bijl, P. K., van Sebille, E., von der Heydt, A. S., Dijkstra, H. A., 2019. Transport Bias by Ocean Currents in Sedimentary Microplankton Assemblages: Implications for Paleoceanographic Reconstructions. *Paleoceanography and Paleoclimatology*, 34(7), 1178-1194.

Nooteboom, P. D., Delandmeter, P., van Sebille, E., Bijl, P. K., Dijkstra, H. A., von der Heydt, A. S., 2020. Resolution dependency of sinking Lagrangian particles in ocean general circulation models. *PLOS ONE*, 15(9), 1-16.

Onink, V., Wichmann, D., Delandmeter, P., van Sebille, E., 2019. The Role of Ekman Currents, Geostrophy, and Stokes Drift in the Accumulation of Floating Microplastic. *Journal of Geophysical Research: Oceans*, 124(3), 1474-1490.

Post, F. H., Van Walsum, T., 1993. Fluid flow visualization. *Focus on Scientific Visualization*, Springer, 1–40.

Raith, F., Rber, N., Haak, H., Scheuermann, G., 2017. Visual Eddy Analysis of the Agulhas Current. K. Rink, A. Middel, D. Zeckzer, R. Bujack (eds), *Workshop on Visualisation in Environmental Sciences (EnvirVis)*, The Eurographics Association.

Schilling, H. T., Everett, J. D., Smith, J. A., Stewart, J., Hughes, J. M., Roughan, M., Kerry, C., Suthers, I. M., 2020. Multiple spawning events promote increased larval dispersal of a predatory fish in a western boundary current. *Fisheries Oceanography*, 29(4), 309-323.

Schroeder, W. J., Lorensen, B., Martin, K., 2004. *The visualization toolkit: an object-oriented approach to 3D graphics*. Kitware.

Shah, S. H. A. M., Heemink, A. W., Deleersnijder, E., 2011. Assessing Lagrangian schemes for simulating diffusion on non-flat isopycnal surfaces. *Ocean Modelling*, 39(3-4), 351–361.

Thyng, K. M., Greene, C. A., Hetland, R. D., Zimmerle, H. M., DiMarco, S. F., 2016. True colors of oceanography: Guidelines for effective and accurate colormap selection. *Oceanography*, 29(3), 9–13.

Tufte, E., 2001. *The Visual Display of Quantitative Information*. Graphics Press.

van Sebille, E., Aliani, S., Law, K. L., Maximenko, N., Alsina, J. M., Bagaev, A., Bergmann, M., Chapron, B., Chubarenko, I., Cózar, A., Delandmeter, P., Egger, M., Fox-Kemper, B., Garaba, S. P., Goddijn-Murphy, L., Hardesty, B. D., Hoffman, M. J., Isobe, A., Jongedijk, C. E., Kaandorp, M. L. A., Khatmullina, L., Koelmans, A. A., Kukulka, T., Laufktter, C., Lebreton, L., Lobelle, D., Maes, C., Martinez-Vicente, V., Maqueda, M. A. M., Poulain-Zarcos, M., Rodríguez, E., Ryan, P. G., Shanks, A. L., Shim, W. J., Suaria, G., Thiel, M., van den Bremer, T. S., Wichmann, D., 2020. The physical oceanography of the transport of floating marine debris. *Environmental Research Letters*, 15(2), 023003.

van Sebille, E., Delandmeter, P., Schofield, J., Hardesty, B. D., Jones, J., Donnelly, A., 2019. Basin-scale sources and pathways of microplastic that ends up in the Galápagos Archipelago. *Ocean Science*, 15(5), 1341–1349.

Van Sebille, E., England, M. H., Froyland, G., 2012. Origin, dynamics and evolution of ocean garbage patches from observed surface drifters. *Environmental Research Letters*, 7(4), 044040.

van Sebille, E., Griffies, S. M., Abernathey, R., Adams, T. P., Berloff, P., Biastoch, A., Blanke, B., Chassignet, E. P., Cheng, Y., Cotter, C. J., Deleersnijder, E., Döös, K., Drake, H. F., Drijfhout, S., Gary, S. F., Heemink, A. W., Kjellsson, J., Koszalka, I. M., Lange, M., Lique, C., MacGilchrist, G. A., Marsh, R., Mayorga Adame, C. G., McAdam, R., Nencioli, F., Paris, C. B., Piggott, M. D., Polton, J. A., Rühs, S., Shah, S. H., Thomas, M. D., Wang, J., Wolfram, P. J., Zanna, L., Zika, J. D., 2018. Lagrangian ocean analysis: Fundamentals and practices. *Ocean Modelling*, 121, 49 - 75.

Van Wijk, J. J., 2002. Image based flow visualization. *Proceedings of the 29th annual conference on Computer graphics and interactive techniques*, 745–754.

Wichmann, D., Delandmeter, P., Dijkstra, H. A., van Sebille, E., 2019a. Mixing of passive tracers at the ocean surface and its implications for plastic transport modelling. *Environmental Research Communications*, 1(11), 115001.

Wichmann, D., Delandmeter, P., van Sebille, E., 2019b. Influence of Near-Surface Currents on the Global Dispersal of Marine Microplastic. *Journal of Geophysical Research: Oceans*, 124(8), 6086-6096.

Wichmann, D., Kehl, C., Dijkstra, H. A., van Sebille, E., 2020. Detecting flow features in scarce trajectory data using networks derived from symbolic itineraries: an application to surface drifters in the North Atlantic. *Nonlinear Processes in Geophysics*, 27(4), 501–518.

Wichmann, D., Kehl, C., Dijkstra, H. A., van Sebille, E., 2021. Ordering of trajectories reveals hierarchical finite-time coherent sets in Lagrangian particle data: detecting Agulhas rings in the South Atlantic Ocean. *Nonlinear Processes in Geophysics*, 28(1), 43–59.

Zhang, W., Wolfe, C. L., Abernathey, R., 2020. Role of Surface-Layer Coherent Eddies in Potential Vorticity Transport in Quasigeostrophic Turbulence Driven by Eastward Shear. *Fluids*, 5(1), 2.